Published in final edited form as:

Plant Biol (Stuttg). 2010 January ; 12(1): 1–12. doi:10.1111/j.1438-8677.2009.00206.x.

Dismantling of *Arabidopsis* thaliana mesophyll cell chloroplasts during natural leaf senescence

I. M. Evans[1], **A. M. Rus**[2], **E. M. Belanger**[2], **M. Kimoto**[2], and **J. A. Brusslan**[2]

[1]Department of Genetics, Yale University School of Medicine, New Haven, CT, USA

[2]Department of Biological Sciences, California State University, Long Beach, CA, USA

Abstract

One of the earliest events in the process of leaf senescence is dismantling of chloroplasts. Mesophyll cell chloroplasts from rosette leaves were studied in *Arabidopsis thaliana* undergoing natural senescence. The number of chloroplasts decreased by only 17% in fully yellow leaves, and chloroplasts were found to undergo progressive photosynthetic and ultrastructural changes as senescence proceeded. In ultrastructural studies, an intact tonoplast could not be visualized, thus, a 35S-GFP::δ-TIP line with a GFP-labeled tonoplast was used to demonstrate that chloroplasts remain outside of the tonoplast even at late stages of senescence. Chloroplast DNA was measured by real-time PCR at four different chloroplast loci, and a fourfold decrease in chloroplast DNA per chloroplast was noted in yellow senescent leaves when compared to green leaves from plants of the same age. Although chloroplast DNA did decrease, the chloroplast/nuclear gene copy ratio was still 31:1 in yellow leaves. Interestingly, mRNA levels for the four loci differed: *psbA* and *ndhB* mRNAs remained abundant late into senescence, while *rpoC1* and *rbcL* mRNAs decreased in parallel to chloroplast DNA. Together, these data demonstrate that, during senescence, chloroplasts remain outside of the vacuole as distinct organelles while the thylakoid membranes are dismantled internally. As thylakoids were dismantled, Rubisco large subunit, Lhcb1, and chloroplast DNA levels declined, but variable levels of mRNA persisted.

Keywords

Chloroplast DNA; chloroplast mRNA; Rubisco; thylakoids; tonoplast; ultrastructure

INTRODUCTION

In plants, whole organ senescence is a normal part of the life cycle. Older leaves become yellow and abscise, with their nutrients being remobilized to the remaining organs of the plant (Hörtensteiner & Feller 2002). In an effort to understand the molecular basis of leaf senescence, stay-green mutants have been isolated and mutant alleles have been identified (Oh *et al.* 1997; Thomas *et al.* 2002). Mutations in the ORE9 F-box protein (Woo *et al.* 2001) and the GmSARK receptor kinase (Li *et al.* 2006b) result in delayed senescence, and

Correspondence. J. Brusslan, Department of Biological Sciences, California State University, 1250 Bellflower Blvd., Long Beach, CA 90840-3702, USA. bruss@csulb.edu.

expression profiling implicates WRKY transcription factors and MAP kinases in the senescence process (Guo *et al.* 2004; Buchanan-Wollaston *et al.* 2005; van der Graaff *et al.* 2006). In addition, epigenetic modifications are likely to contribute to senescence, as overexpression of an AT-hook protein results in a strong staygreen phenotype (Lim *et al.* 2007). Additional staygreen mutants affect chloroplast processes. *ore4-1* is a weak allele of *pRPS17*, which encodes a plastid ribosomal protein that results in a small (24%) decrease in leaf growth (Woo *et al.* 2002). This mutation is thought to be similar to numerous animal mutants, where a reduced metabolic rate extends longevity. Reduced carbohydrate levels are thought to prolong senescence in Rubisco antisense mutants (Miller *et al.* 2000). *Sgr* encodes a novel plastid protein that is essential for light harvesting complex protein degradation (Park *et al.* 2007) and subsequent Chl catabolism (Hörtensteiner 2006). Although the staygreen mutants have provided clues to the signaling pathways for senescence, they have provided little information on the role of the chloroplast in senescence.

Chloroplasts are reported to breakdown early in the senescence process, prior to the loss of the mitochondria and nucleus (Lim *et al.* 2007). There have been some reports suggesting that chloroplasts are brought into the vacuole, where they are degraded (Wittenbach *et al.* 1982; Minamikawa *et al.* 2001), but other studies indicate that chloroplasts are dismantled internally, with a progressive loss in electron transport and Rubisco activity (Woolhouse 1984). Ultrastructural studies show persisting chloroplasts near the periphery of the cell, but the tonoplast is often ruptured, and it is not possible to determine if the chloroplast is outside of the vacuole (Hurkman 1979; Thomson & Platt-Aloia 1987).

Accumulation of plastoglobuli in chloroplasts of senescent leaves is observed in transmission electron micrographs (Barton 1966; Freeman *et al.* 1978; Hurkman 1979). Tomographic analysis indicates that plastoglobuli remain attached to thylakoid membranes, where they function in lipid biosynthesis and storage (Austin *et al.* 2006). Consistent with this proposed function, the plastoglubuli proteome contains enzymes involved in isoprenoid metabolism as well as structural fibrillins (Ytterberg *et al.* 2006). Plastoglobuli may function during regreening, when the lamellar system redifferentiates (Krupinska 2006). The pathways leading to plastoglobuli formation during senescence have not been clearly defined in previous studies because researchers often use different species under different senescence conditions (Krupinska 2006).

As thylakoid membranes are dismantled, photosynthesis declines. The cytochrome b_6/f complex is degraded first, and PSII activity decreases later. PSII photochemical efficiency (Fv /Fm) and the D1 protein are retained in leaves in which 75% of the Chl has been degraded (Guiamet *et al.* 2002). During senescence, the timing of chloroplast DNA degradation has not been established. Chloroplast DNA has been reported to be absent from chloroplasts isolated from mature leaves of *Arabidopsis* (Rowan *et al.* 2004) and maize (Oldenburg & Bendich 2004), and more recently white and blue light were shown to stimulate the degradation of chloroplast DNA in maize (Oldenburg *et al.* 2006) and *Medicago truncatula* seedlings (Shaver *et al.* 2008). A separate study questioned these findings, with the demonstration that chloroplast DNA levels remained constant in mature *Arabidopsis* rosette, cauline, and even in senescent rosette leaves (Li *et al.* 2006b). Plastid

DNA copy number was also measured by real-time qPCR throughout cotyledon, rosette leaf, and cauline leaf development, and found to be constant, even in older leaves in which the Fv /Fm ratio was slightly decreased (Zoschke *et al.* 2007).

In an effort to address some of the unresolved issues in leaf senescence, chloroplast number and ultrastructure were observed in *Arabidopsis* leaves at various stages of senescence. Our results indicate that chloroplast number declined slightly, while a dramatic, but ordered, internal reorganization of the chloroplast occurred within the organelle. In addition, a transgenic line with a GFP-labeled tonoplast was used to demonstrate that chloroplasts remain at the periphery of the cell, outside of the tonoplast, late into the process of senescence. Chloroplast DNA and mRNA levels were also measured for four chloroplast genes and compared to a nuclear control gene using real-time qPCR.

MATERIALS AND METHODS

Plant growth

Arabidopsis thaliana ecotype Col-0 was grown in soil (Sunshine Mix LC1) under continuous white light (70 μmoles photons $m^{-2} \cdot s^{-1}$), and watered weekly with dilute Miracle Gro. After 7–8 weeks of growth, rosettes were removed from the soil, and senescent tissue at the base of the rosette was pooled into zones (Fig. 1A). The 35S-GFP::δ-TIP line was obtained from Dr Natasha Raikhel at University of California, Riverside.

Chloroplast number per cell area

Tissue was fixed and observed by difference interference contrast microscopy as described (Pyke & Leech 1991). Chloroplasts were counted in two separate planes for each cell to estimate chloroplasts at the top and bottom surface of each cell. Images from at least 20 cells from each sample were digitized, and cell area was quantified by NIH ImageJ software (developed at the US National Institutes of Health and available on the Internet at http://rsb.info.nih.gov/nih-image/).

Transmission electron microscopy

Leaf tissue from each zone was fixed whole in 5% (v /v) glutaraldehyde in Sorensen's phosphate buffer, pH 7.2. Leaves were sectioned into 1-mm wide strips while submerged in glutaraldehyde. Sections were stored at 4 °C. Serial dehydrations in 30%, 50%, 75%, 95%, and 100% ethanol were performed, followed by four 15-min washes with propylene oxide. Araldite 502 resin was used to embed samples in flat molds. Thick sections (*ca*. 400 nm), obtained using a Porter-Blum MT-2 ultramicrotome, were stained with 0.5% toluidine blue in 1% borax. Thin sections, obtained using an Ultratome Nova, were stained with saturated aqueous lead citrate and uranyl acetate. Transmission electron micrographs were obtained using a Joel 1200 Ex II electron microscope. Fifty individual chloroplasts were scored from each zone to determine distribution of chloroplast types at different stages of senescence.

Chl and Fv /Fm

Leaves were sliced into thin strips and then incubated overnight at room temperature in the dark in *N*,*N*'-dimethylformamide (DMF) for complete elution of Chl. Absorbance was

recorded at 647 and 664 nm, and total Chl was calculated from published extinction coefficients (Porra *et al*. 1989). Chl levels were normalized to fresh weight of well-watered plants prior to harvest. Fv/Fm was measured using a Z990 FluoroPen (Qubit Systems, Kingston, Ontario, Canada).

Immunoblots

Total proteins were extracted as described previously (Harper *et al.* 2004). Ten microgram of total protein extract was loaded on 11% SDS-PAGE gels. Gels were run at 30 mA for 30 min, followed by 60 mA for 1 h, and then transferred to nitrocellulose at 25 V overnight in carbonate buffer (3 mm sodium carbonate, 10 mm sodium bicarbonate, 10% methanol, pH 9.9). Direct Blue-71 staining was performed to ensure equal protein loading in each lane (Hong *et al.* 2000). Nitrocellulose filters were incubated overnight with a 1/1000 titer of primary antibody raised against one protein, but found to have high specificity for Rubisco LSU (raised in rabbit). Anti-Lhcb1 (Agrisera, Sweden) was used at a titer of 1/10,000. The secondary antibody against rabbit IgG was conjugated to alkaline phosphatase (raised in goat, Sigma-Aldrich, St. Louis, MO, USA). AP staining was done with NBT and BCIP. DB-71 stained and immunoreacted blots were scanned and pixels were quantified using NIH ImageJ Software. Immunoreacted signal was normalized to the DB-71 signal.

Real-time qPCR

Genomic DNA was isolated using DNAzol according to manufacturer's instructions except that volumes were decreased by 50% (Invitrogen Inc., Carlsbad, CA, USA). RNA was isolated using Trizol reagent (Invitrogen), and cDNA was synthesized using random hexamers (Operon Biotechnologies Inc., Huntsvill, AL, USA) and MMLV reverse transcriptase (Promega Corp., Madison, WI, USA). cDNA was diluted 1:4 prior to real-time PCR. Real time PCR amplification was performed in an MX3000P real-time PCR machine (Stratagene, Cedar Creek, TX, USA) using 2× SYBR Green mix (AB Gene, Epsom, UK) in a total volume of 12 μl. PCR reactions all used a 57 °C annealing temperature, and dissociation curves were done to check for primer dimers. The primers were as follows: ACT2-F 5′GGCGACTTGACAGAGAAGAa, ACT2-R 5′TGGAAAGAAAGAGCGGAAGA, psbA-F 5′AACTAAGTTCCCACTCACGA, psbA-R 5′CATCCGTTGATGAATGGCTA, rpoC1-F 5′CCACGGCTTCTTGTACCAAT, rpoC1-R 5′TTCTTCCTCCCGAGTTGAGA, rbcL-F 5′TACCTGGTGTTCTGCCTGTG, rbcL-R 5′GCTACTCGGTTGGCTACGG, ndhB-F 5′CCTGACCCTGCTTCACCTTA, ndhB-R 5′TAGCCCCTTCTCATCAATGG.

Laser scanning confocal microscopy and DAPI staining

For the 35S-GFP::δ-TIP line, a small region of leaf tissue was placed on a microscope slide on a drop of water, and covered with a cover slip. For DAPI staining, thin leaf sections were vacuum infiltrated with 0.6% glutaraldehyde for 4 min, incubated overnight at 4 °C, and then incubated in 1 μg /ml 4′,6-diamidino-2-phenylindole dihydrochloride (DAPI) for 30 min at 25 °C in the dark prior to confocal microscopy. Mesophyll cells were viewed on an Olympus Fluoroview 1000 confocal laser scanning system at 20× (NA 0.75, WD 0.65 mm) with argon ion laser excitation of DAPI at 405 nm, GFP at 488 nm, and Chl at 559 nm.

Fluorescence emission was detected from 425–475 nm for DAPI, 498–525 nm for GFP, and 618–718 nm for Chl.

RESULTS

Zoning system for leaf senescence

In order to study leaf senescence on a population of individual *Arabidopsis* plants, a zoning system was developed that would allow for tissue collection after 7–8 weeks of growth, when multiple bolts were well developed and natural senescence was occurring in the leaves at the base of the rosette. Zone 3 leaves were mature rosette leaves that were still green, while Zone 1 tissue had lost nearly all Chl and appeared yellow. Zone 2 tissue was intermediate between Zone 3 and Zone 1 (Fig. 1A). Total Chl measurements (n = 8) indicated a steady loss of pigments in each zone (Fig. 1B). Green tissue was isolated from mature leaves after 4 weeks of growth, and had significantly more Chl than all zones collected from 8-week-old plants. Photosystem II photochemical efficiency (measured as Fv /Fm, n = 3) also decreased during senescence, but not at the same rate as Chl loss (Fig. 1C). Total proteins were extracted from zoned leaf tissue and stained with Direct Blue-71 (DB-71) after transfer to nitrocellulose. Filters were immunoreacted with antibodies to the Rubisco large subunit and Lhcb1 (Fig. 1D). A steady loss of Rubisco was observed, with 58% remaining in Zone 1 compared to Zone 3. Lhcb1 declined more slowly, and was 81% as abundant in Zone 1 as in Zone 3. The relatively small decline in chloroplast protein levels observed is likely due to loading on a per protein basis rather than on a per leaf area basis. Together, these observations suggested that this zoning system captured the normal process of leaf senescence.

Chloroplast number in senescent zones

Leaf tissue from each zone was fixed and then visualized by differential interference contrast (DIC) microscopy to count chloroplasts per cell area (Pyke & Leech 1991). Chloroplasts were highly abundant in green tissue and in all zones (Fig. 2A). In green tissue, the chloroplasts were most distinct. Chloroplasts were counted and normalized per cell area (Fig. 2B, n = 16). Two sample *t*-tests were used to determine if chloroplast counts were significantly different between any two regions. Green and Zone 3 were not significantly different (P = 0.212) and, similarly, Zone 2 and Zone 1 were not significantly different (P = 0.301); however, Zone 2 and Zone 1 had significantly less chloroplasts per leaf area than green and Zone 3 (P = 0.0027 for green *versus* Zone 2, P = 0.0032 for green *versus* Zone 1, P = 0.0082 for Zone 3 *versus* Zone 2, and P = 0.0089 for Zone 3 *versus* Zone 1). Although significantly different, the number of chloroplasts in Zone 2 and Zone 1 tissues was reduced by only 17% compared to green and Zone 3 tissues. This contrasts to the much greater loss of Chl, photosytem II photochemical efficiency, and Rubisco LSU protein.

Ultrastructural changes during leaf senescence

Transmission electron microscopy was used to track ultrastructural changes as senescence proceeded. Representative chloroplasts from each stage are shown in Figs 3 and 4. Figure 3A shows a healthy chloroplast from green tissue, with stacked thylakoid membranes separated by stromal lamellae, a prominent starch granule, and an intact double chloroplast

membrane. Zone 3 chloroplasts had swirled thylakoid membranes, but starch granules were still present (Fig. 3B, top arrow). Thylakoid membranes began to loosen in Zone 2 tissue, and large folds of membranes are visible in Fig. 3C, and at higher magnification in Fig. 3D. Similar loose folds were observed in dark-induced artificial senescence in detached wheat leaves (Hurkman 1979). TEM micrographs of Zone 1 tissue are shown in Fig. 4. The loose membrane folds became less prevalent, while plastoglobuli increased in abundance, and chloroplasts transitioned into gerontoplasts (Krupinska 2006). The circularization of the loose membrane folds and increased density of these coalesced membranes is apparent in Fig. 4B and the higher magnification view highlighted by asterisks in Fig. 4C, suggesting that plastoglobuli formed from the loose folds during senescence. A circular chloroplast with few plastoglobuli and membrane swirls represents the final stage of senescence (Fig. 4D). At this time, mitochondria can be seen flanking the chloroplast. Fifty chloroplasts, randomly chosen from TEM micrographs at each stage, were scored as healthy, swirled thylakoids, loose thylakoid folds, or plastoglobuli. Figure 4E shows that thylakoid membrane dismantling followed an orderly process, with green tissue having healthy chloroplasts, Zone 3 predominantly swirled thylakoids, Zone 2 predominantly loose folds, while Zone 1 was predominantly plastoglobuli. This quantitative analysis demonstrates an ordered sequence of ultrastructural changes leading to gerontoplast formation in naturally senescing *Arabidopsis* leaves.

Because the tonoplast is difficult to discern in TEM micrographs, a 35S-GFP::δ-TIP fusion line (Cutler *et al.* 2000; Avila *et al.* 2003) was observed with laser scanning confocal microscopy to determine if the chloroplasts remain outside of the tonoplast during senesence. Chloroplasts were visualized by autofluorescence, while the tonoplast was labeled with GFP. The tonoplast contours the interior side of chloroplasts in green tissue (Fig. 5A–C). In Zone 1 tissue, the tonoplast GFP fluorescence is less bright and distinct, but folding around the interior sides of chloroplasts is observed in the plane of focus indicated by the asterisks (Fig. 5D–F). These images demonstrate that chloroplasts remain outside of the vacuole late into senescence in yellow Zone 1 leaves.

Chloroplast DNA and mRNA levels during leaf senescence

Total DNA was isolated from Zone 3, Zone 2, and Zone 1 tissue. DNA was separated by electrophoresis to estimate relative DNA concentration, and then subject to real-time PCR to quantify *psbA, rbcL, ndhB, rpoC1*, and *ACT2* DNA levels. The first four genes are located on different regions of the chloroplast genome, while *ACT2* is a nuclear gene (Table 1). In all cases, chloroplast genes amplified at least five cycles earlier than the nuclear gene control. For $2^{-\Delta\Delta CT}$ analysis, chloroplast DNA levels were normalized to the nuclear *ACT2* reference and then compared to the Zone 3 calibrator (Livak & Schmittgen 2001). The data shown in Fig. 6A demonstrate that, compared to Zone 3 leaves, Zone 2 leaves had 80%, while Zone 1 leaves had only 20% chloroplast DNA at all four loci. In Zone 1, chloroplast numbers decreased by 17%, thus chloroplast DNA on a per chloroplast basis had decreased fourfold. An estimate of chloroplast/nuclear gene copy number was made by calculating the $2^{-\Delta CT}$ in Zone 3 and Zone 1, using the C_T values for *psbA* and *ACT2*. The chloroplast / nuclear ratio was 84 for Zone 3, which decreased to 31 for Zone 1, demonstrating that

chloroplast DNA copy number remains significantly above nuclear DNA copy number, even in Zone 1 tissue.

Plastid mRNA levels were also measured by real-time qPCR (Fig. 6B). *rpoC1*, encoding chloroplast RNA polymerase, and *rbcL*, encoding the large subunit of Rubisco, were found to decrease in parallel with chloroplast DNA levels. However, *psbA*, encoding the D1 core reaction center protein of photosystem II, and *ndhB*, encoding NAD(P)H dehydrogenase, which functions in cyclic electron flow around PSI (Shikanai *et al.* 1998), did not decline as much, and were between 60–75% as abundant in Zone 1 as in Zone 3. The maintenance of *psbA* and *ndhB* mRNA could result from increased expression or increased stability. *psbA* mRNA has a $t_{1/2}$ of more than 40 h (Kim *et al.* 1993). This relatively long half-life suggests that *psbA* mRNA persisted because it was not degraded. *ndhB* mRNA $t_{1/2}$ has not been reported.

Several studies have used DAPI staining of protoplasts or purified chloroplasts to detect chloroplast DNA (James & Jope 1978; Sodmergen *et al.* 1991; Rowan *et al.* 2004). To determine whether chloroplast DNA could be detected with DAPI in intact mature leaves, Zone 3 leaves from 7-week-old plants were sliced into thin sections and fixed in 0.6% glutaraldehyde, and then stained with DAPI (1 μg /ml). Confocal microscopy demonstrated strong staining in nuclei, but chloroplasts were not convincingly stained, although faint staining was observed at the periphery and outside of the chloroplasts (Fig. 7). The strong nuclear staining indicated that our procedure allowed DAPI to infiltrate the mesophyll cells; however the lack of DAPI fluorescence in mature leaf chloroplasts suggests that these organelles are not DAPI permeable, and demonstrates that DAPI staining is not an appropriate technique for measuring chloroplast DNA in mature tissue.

DISCUSSION

The fate of chloroplasts during natural leaf senescence has been described in the dicot model plant, *Arabidopsis thaliana*. This comprehensive study demonstrates that chloroplast numbers are only slightly decreased, and that chloroplasts are retained outside of the vacuole. In addition, our analysis of ultrastructure demonstrates that thylakoids follow a sequential dismantling. Chloroplasts were dismantled internally during leaf senescence concomitant to the loss of photosynthetic function, but were only 17% less abundant in Zones 1 and 2 compared to mature green leaves. This is similar to the 20% reduction in chloroplast number observed during leaf senescence in wheat (Ono *et al.* 1995). The 35S-GFP::δ-TIP line allowed visualization of the tonoplast wrapped around the periphery of chloroplasts even in yellow leaves, demonstrating that chloroplasts remain outside of the vacuole. This observation does not exclude the possibility that certain plastid components could be degraded in the vacuole, but demonstrates that whole chloroplasts are not being transported into the vacuole for degradation, as suggested previously (Wittenbach *et al.* 1982; Minamikawa *et al.* 2001). As senescence proceeded, progressive internal reorganization began with swirling of thylakoid membranes into loose, large folded structures that then circularized into plastoglobuli. As these changes occurred, the chloroplasts remained distinct organelles.

As leaf senescence proceeded, Chl levels decreased and photochemical efficiency of photosystem II and Rubisco protein levels also declined, but more slowly. Thus, even in Zone 2 tissue, in which Chl is decreased by nearly 70%, Fv/Fm was reduced by only 27% when compared with mature green leaves (Fig. 1C), Rubisco and Lhcb1 were still present (Fig. 1D), and starch granules could be observed (Fig. 3C). In yellow, Zone 1 tissue, Fv /Fm levels dropped to 0.12, indicating that chloroplasts in Zone 1 were mostly photosynthetically inactive.

Our findings show the chloroplast DNA decreased fourfold in Zone 1. Zn-dependent chloroplast-localized nucleases have previously been implicated in cpDNA degradation in rice (Sodmergen *et al.* 1991) and may be the cause of the loss of cpDNA that was observed here. Although cpDNA levels do decrease, the ratio of chloroplast /nuclear gene copies was 31 /1 in Zone 1. Our sampling included later stages of leaf senescence than a previous study that found that cpDNA levels remained constant throughout cotyledon, rosette, and cauline leaf development (Zoschke *et al.* 2007). In the previous study, the oldest rosette leaves sampled (Ros 50 /8) had Fv /Fm values of 0.77, while our Zone 1 tissue had an Fv/Fm value of 0.12.

In mature green leaves isolated from 7-week-old plants, chloroplasts could not be stained by DAPI under conditions where nuclei were readily stained. Abundant levels of cpDNA in mature leaves have been observed in previous studies that used gel blot analysis to quantify chloroplast and mitochondrial DNA (Li *et al.* 2006a) or qPCR of various chloroplast genes (Zoschke *et al.* 2007). Other studies have shown that percoll gradient-purified chloroplasts from developing *Arabidopsis* 7-day-old rosette leaves stained with DAPI, but that chloroplasts isolated from mature green leaves (38-day-old) did not stain with DAPI (Rowan *et al.* 2004). This same group concluded that loss of cpDNA in mature leaves is a normal part of chloroplast development (Oldenburg & Bendich 2004; Rowan *et al.* 2004; Oldenburg *et al.* 2006; Shaver *et al.* 2008); however, it is more likely that DAPI stain does not infiltrate chloroplasts in mature leaves, since our work and two additional studies (Li *et al.* 2006a; Zoschke *et al.* 2007) using well-established molecular methods, have found high levels of cpDNA in mature leaves. These studies both discussed the possibility that DAPI staining of isolated chloroplasts may not be an appropriate method for estimating chloroplast DNA levels, and suggested that the isolation procedure may have resulted in the loss of chloroplast DNA from mature tissue. Our inability to convincingly stain chloroplasts in intact tissue, under conditions where nuclei stained brightly, demonstrates that mature chloroplasts are not highly permeable to DAPI.

In yellow Zone 1 leaf tissue, *psbA* and *ndhB* mRNA persisted. For *psbA* mRNA, this is likely a result of high mRNA stability, since *psbA* transcription is reduced by approximately 50% in early stages of senescence (Zoschke *et al.* 2007). The half-life of *ndhB* mRNA has not been reported, so the mechanism of persistence for this plastid transcript is not known. The physiological relevance of retaining *ndhB* mRNA is unclear, since photosystem I cyclic electron flow requires a functioning cytochrome b_6/f complex, and this complex degrades early in the process of senescence (Guiamet *et al.* 2002). Similarly, *psbA* mRNA levels remained abundant in Zone 1 tissue when PSII photochemical efficiency was greatly

decreased (Fig. 1C). The *psbA* mRNA is likely still functional, as soybean leaf disks that had lost 70% of their Chl were still able to synthesize the D1 protein (Guiamet *et al.* 2002).

Figure 1D shows that the large subunit of Rubisco is nearly completely degraded in Zone 1 tissue, in which most chloroplasts remain as distinct organelles outside of the vacuole. Chloroplast proteins comprise 75% of cellular protein (Dalling 1987), yet the mechanisms for degradation of chloroplast proteins have not yet been defined. There have been reports of partial Rubisco degradation in intact chloroplasts (Roulin & Feller 1998; Kokubun *et al.* 2002), but activities have not been robust and corresponding proteases have not been identified. Senescence-associated vacuoles (SAVs) rich in cysteine proteases have been isolated from senescent mesophyll cells and likely play a role in chloroplast proteolysis (Otegui *et al.* 2005; Martinez *et al.* 2008a). In addition, Rubisco-containing bodies (RCBs) have been observed in the cytoplasm of senescent wheat leaves (Chiba *et al.* 2003) and nutrient-deprived *Arabidopsis* leaves (Ishida *et al.* 2008a). RCBs do not form in *atg5* autophagy mutants, which undergo accelerated senescence, suggesting that chloroplast protein degradation is not strictly dependent on RCBs (Ishida *et al.* 2008b). Chloroplast proteases may also play a role during senescence (Feller *et al.* 2008; Martinez *et al.* 2008b), and the genomic tools available to the *Arabidopsis* research community could be used to determine which, if any, chloroplast proteases are important.

This comprehensive study describes the fate of chloroplasts during natural leaf senescence in *Arabidopsis thaliana*. Using a combination of DIC, TEM, and confocal microscopy, the chloroplast number was shown to decline slightly, with the remaining chloroplasts following an orderly dismantling of thylakoid membranes, while remaining outside of the vacuole, flanked by the tonoplast. In addition, as senescence progressed, photochemical efficiency, as well as the levels of Rubisco LSU, Lhcb1, and cpDNA, decreased, while cpRNAs varied in abundance.

ACKNOWLEDGEMENTS

We would like to thank Tom Douglass for his guidance in transmission electron microscopy, Simon Malcomber for helpful discussions and Natasha Raikhel for providing the 35S-GFP::δ-TIP line. Finance for this study was provided by the National Science Foundation (RUI 0415108) to JAB and (DBI 0722757) to the Department of Biological Sciences for confocal equipment grant, an HHMI Undergraduate Research Award to IME, a LSAMP (NSF HRD-0331537) to IME, and a Graduate Research Fellowship (CSULB Provost) to MK.

REFERENCES

Austin JR, Frost E, Vide P-A, Kessler F, Staehelin LA. Plastoglobules are lipoprotein subcompartments of the chloroplast that are permanently coupled to thylakoid membranes and contain biosynthetic enzymes. Plant Cell. 2006; 18:1693–1703. [PubMed: 16731586]

Avila EL, Zouhar J, Agee AE, Carter DG, Chary NS, Raikhel NV. Tools to study plant organelle biogenesis. Point mutation lines with disrupted vacuoles and high-speed confocal screening of green fluorescent protein-tagged organelles. Plant Physiology. 2003; 133:1673–1676. [PubMed: 14681530]

Barton R. Fine structure of mesophyll cells in senescing leaves of *Phaseolus*. Planta. 1966; 71:314–325. [PubMed: 24554106]

Buchanan-Wollaston V, Page T, Harrison E, Breeze E, Lim PO, Nam HG, Lin J-F, Wu S-H, Swidzinski J, Ishizaki K, Leaver CJ. Comparative transcriptome analysis reveals significant differences in gene expression and signalling pathways between developmental and dark /

starvation- induced senescence in *Arabidopsis*. Plant Journal. 2005; 42:567–585. [PubMed: 15860015]

Chiba A, Ishida H, Nishizawa NK, Makino A, Mae T. Exclusion of ribulose-1,5-bisphosphate carboxylase / oxygenase from chloroplasts by specific bodies in naturally senescing leaves of wheat. Plant and Cell Physiology. 2003; 44:914–921. [PubMed: 14519773]

Cutler SR, Ehrhardt DW, Griffiths JS, Somerville CR. Random GFP::cDNA fusions enable visualization of subcellular structures in cells of *Arabidopsis* at a high frequency. Proceedings of the National Academy of Sciences USA. 2000; 97:3718–3723.

Dalling, MJ. Proteolytic enzymes and leaf senescence. In: Thomson, WW.; Nothnagel, EA.; Huffaker, RC., editors. Plant Senescence: Its Biochemistry and Physiology. Rockville, MD: American Society of Plant Physiologists; 1987. p. 54-70.

Feller U, Anders I, Mae T. Rubiscolytics: fate of Rubisco after its enzymatic function in a cell is terminated. Journal of Experimental Botany. 2008; 59:1615–1624. [PubMed: 17975207]

Freeman BA, Platt-Aloia K, Mudd JB, Thomson WW. Ultrastructural and lipid changes associated with the aging of citrus leaves. Protoplasma. 1978; 94:221–233.

van der Graaff E, Schwacke R, Schneider A, Disimone M, Flügge U-I, Kunze R. Transcription analysis of *Arabidopsis* membrane transporters and hormone pathways during developmental and induced leaf senescence. Plant Physiology. 2006; 141:776–792. [PubMed: 16603661]

Guiamet JJ, Tyystjarvi E, John I, Kairavuo M, Pichersky E, Nooden LD. Photoinhibition and loss of photosystem II reaction center proteins during senescence in soybean leaves. Enhancement of photoinhibition by the ‘‘stay-green’’ mutation cytG. Physiologia Plantarum. 2002; 115:468–478. [PubMed: 12081540]

Guo Y, Cai Z, Gan S. Transcriptome of *Arabidopsis* leaf senescence. Plant, Cell and Environment. 2004; 27:521–549.

Harper AL, von Gesjen SE, Linford AS, Peterson MP, Faircloth RS, Thissen MM, Brusslan JA. Chlorophyllide *a* oxygenase mRNA and protein levels correlate with the chlorophyll *a/b* ratio in *Arabidopsis thaliana*. Photosynthesis Research. 2004; 79:149–159. [PubMed: 16228389]

Hong H-Y, Yoo G-Y, Choi J-K. Direct Blue 71 staining of proteins bound to blotting membranes. Electrophoresis. 2000; 21:841–845. [PubMed: 10768767]

Hörtensteiner S. Chlorophyll degradation during senescence. Annual Review of Plant Biology. 2006; 57:55–77.

Hörtensteiner S, Feller U. Nitrogen metabolism and remobilization during senescence. Journal of Experimental Botany. 2002; 53:927–937. [PubMed: 11912235]

Hurkman WJ. Ultrastructural changes of chloroplasts in attached and detached, aging primary wheat leaves. American Journal of Botany. 1979; 66(1):64–70.

Ishida, H.; Yoshimoto, K.; Reisen, D.; Makino, A.; Ohsumi, Y.; Hanson, MR.; Mae, T. Visualization of rubisco-containing bodies derived from chloroplasts in living cells of *Arabidopsis*. In: Allen, JF.; Gantt, E.; Gohlbeck, JH.; Osmond, B., editors. Photosynthesis. Energy from the Sun: 14 th International Congress on Photosynthesis. New York: Springer; 2008a. p. 1213-1216.

Ishida H, Yoshimoto K, Izumi M, Reisen D, Yano Y, Makino A, Ohsumi Y, Hanson MR, Mae T. Mobilization of Rubisco and stroma-localized fluorescent proteins of chloroplasts to the vacuole by an *ATG* gene-dependent autophagic process. Plant Physiology. 2008b; 148:142–155. [PubMed: 18614709]

James TW, Jope C. Visualization by fluorescence of chloroplast DNA in higher plants by means of the DNA-specific probe 4’6-diamidino-2-phenylindole. Journal of Cell Biology. 1978; 79:623–630. [PubMed: 730764]

Kim M, Christopher DA, Mullet JE. Direct evidence for selective modulation of psbA, rpoA, rbcL and 16S RNA stability during barley chloroplast development. Plant Molecular Biology. 1993; 22:447–463. [PubMed: 8329684]

Kokubun N, Ishida H, Makino A, Mae T. The degradation of the large subunit of ribulose-1,5-bisphosphate carboxylase / oxygenase into the 44-kDa fragment in the lysates of chloroplasts incubated in darkness. Plant and Cell Physiology. 2002; 43:1390–1395. [PubMed: 12461140]

Krupinska, K. Fate and activities of plastids during leaf senescence. In: Wise, RR.; Hoober, JK., editors. The Structure and Function of Plastids. The Netherlands: Springer; 2006. p. 433-449.

Li W, Ruf S, Bock R. Constancy of organellar genome copy numbers during leaf development and senescence in higher plants. Molecular and Genetic Genomics. 2006a; 275:185–192.

Li X-P, Gan R, Li P-L, Ma Y-Y, Zhang L-W, Zhang R, Wang Y, Wang NN. Identification and functional characterization of a leucine-rich repeat receptor-like kinase gene that is involved in regulation of leaf senescence. Plant Molecular Biology. 2006b; 61:829–844. [PubMed: 16927199]

Lim PO, Kim HJ, Nam HG. Leaf senescence. Annual Review of Plant Biology. 2007; 58:115–136.

Livak KJ, Schmittgen TD. Analysis of relative gene expression data using real-time quantitative PCR and the 2^{-DDCT} method. Methods. 2001; 25:402–408. [PubMed: 11846609]

Martinez DE, Costa ML, Gomez FM, Otegui MS, Guiamet JJ. 'Senescence-associated vacuoles' are involved in the degradation of chloroplast proteins in tobacco leaves. The Plant Journal. 2008a; 56:196–206. [PubMed: 18564383]

Martinez DE, Costa ML, Guiamet JJ. Senescence-associated degradation of chloroplast proteins inside and outside the organelle. Plant Biology. 2008b; 10:15–22. [PubMed: 18721308]

Miller A, Schlagnhaufer C, Spalding M, Rodermel S. Carbohydrate regulation of leaf development: prolongation of leaf senescence in Rubisco antisense mutants of tobacco. Photosynthesis Research. 2000; 63:1–8. [PubMed: 16252160]

Minamikawa T, Toyooka K, Okamoto T, Hara-Nishimura I, Nishimura M. Degradation of ribulose-bisphosphate carboxylase by vacuolar enzymes of senescing French bean leaves: immunocytochemical and ultrastructural observations. Protoplasma. 2001; 218:144–153. [PubMed: 11770431]

Oh AS, Park J-H, Lee GI, Paek HP, Park SK, Nam HG. Identification of three genetic loci controlling leaf senescence in *Arabidopsis thaliana*. Plant Journal. 1997; 12:527–535. [PubMed: 9351240]

Oldenburg DJ, Bendich AJ. Changes in the structure of DNA molecules and the amount of DNA per plastid during chloroplast development in maize. Journal of Molecular Biology. 2004; 344:1311–1330. [PubMed: 15561145]

Oldenburg DJ, Rowan BA, Zhao L, Walcher CL, Schleh M, Bendich AJ. Loss or retention of chloroplast DNA in maize seedlings is affected by both light and genotype. Planta. 2006; 225:41–55. [PubMed: 16941116]

Ono K, Hashimoto H, Katoh S. Changes in the number and size of chloroplasts during senescence of primary leaves of wheat grown under different conditions. Plant and Cell Physiology. 1995; 36:9–17.

Otegui MS, Noh Y-S, Martinez DE, Vila Petroff MG, Staehelin LA, Amasino RM, Guiamet JJ. Senescence- associated vacuoles with intense proteolytic activity develop in leaves of *Arabidopsis* and soybean. Plant Journal. 2005; 41:831–844. [PubMed: 15743448]

Park S-Y, Yu J-W, Park J-S, Li J, Yoo S-C, Lee N-Y, Lee S-K, Jeong S-W, Seo HS, Koh H-J, Jeon J-S, Park Y-I, Paek N-C. The senescence-induced staygreen protein regulates chlorophyll degradation. Plant Cell. 2007; 19:1649–1664. [PubMed: 17513504]

Porra RJ, Thompson WA, Kriedemann PE. Determination of accurate extinction coefficients and simultaneous equations for assaying chlorophylls *a* and *b* extracted with four different solvents: verification of the concentration of chlorophyll standards by atomic absorption spectroscopy. Biochimica et Biophysica Acta. 1989; 975:384–394.

Pyke KA, Leech RM. Rapid image analysis screening procedure for identifying chloroplast number mutants in mesophyll cells of *Arabidopsis thaliana* (L.) Heynh. Plant Physiology. 1991; 96:1193–1195. [PubMed: 16668319]

Roulin S, Feller U. Light-independent degradation of stromal proteins in intact chloroplasts isolated from *Pisum sativum* L. leaves: requirement for divalent cations. Planta. 1998; 205:297–304.

Rowan BA, Oldenburg DJ, Bendich AJ. The demise of chloroplast DNA in *Arabidopsis*. Current Genetics. 2004; 46:176–181. [PubMed: 15249983]

Shaver JM, Oldenburg DJ, Bendich AJ. The structure of chloroplast DNA molecules and the effects of light on the amount of chloroplast DNA during development of *Medica-go truncatula*. Plant Physiology. 2008; 146:1064–1074. [PubMed: 18218970]

Shikanai T, Endo T, Hashimoto T, Yamada Y, Asada K, Yokota A. Directed disruption of the tobacco *ndhB* gene impairs cyclic electron flow around photosystem I. Proceedings of the National Academy of Sciences of the United States of America. 1998; 95:9705–9709. [PubMed: 9689145]

Sodmergen S, Kawano S, Tano S, Kuroiwa T. Degradation of chloroplast DNA in second leaves of rice (*Oryza sativa*) before leaf yellowing. Protoplasma. 1991; 160:89–98.

Thomas H, Ougham H, Canter P, Donnison I. What stay-green mutants tell us about nitrogen remobilization in leaf senescence. Journal of Experimental Botany. 2002; 53:801–808. [PubMed: 11912223]

Thomson, WW.; Platt-Aloia, KA. Ultrastructure and senescence in plants. In: Thomson, WW.; Nothnagel, EA.; Huffaker, RC., editors. Plant Senescence: Its Biochemistry and Physiology. Rockville, MD: American Society of Plant Physiologists; 1987. p. 20-30.

Wittenbach VA, Lin W, Herbert RR. Vacuolar localization of proteases and degradation of chloroplasts in mesophyll protoplasts from senescing primary wheat leaves. Plant Physiology. 1982; 69:98–102. [PubMed: 16662193]

Woo RH, Chung KM, Park J-H, Oh AS, Ahn T, Hong SH, Jang SK, Nam HG. ORE9, an F-box protein that regulates leaf senescence in *Arabidopsis*. Plant Cell. 2001; 13:1779–1790. [PubMed: 11487692]

Woo RH, Goh C-H, Park J-H, de la Serve BT, Kim J-H, Park Y-I, Nam HG. Extended leaf longevity in the *ore4-1* mutant of *Arabidopsis* with a reduced expression of a plastid ribosomal protein gene. Plant Journal. 2002; 31:331–340. [PubMed: 12164812]

Woolhouse HW. The biochemistry and regulation of senescence in chloroplasts. Canadian Journal of Botany. 1984; 62:2934–2942.

Ytterberg AJ, Peltier J-B, van Wijk KJ. Protein profiling of plastoglobules in chloroplasts and chromoplasts. A surprising site for differential accumulation of metabolic enzymes. Plant Physiology. 2006; 140:984–997. [PubMed: 16461379]

Zoschke R, Liere K, Borner T. From seedling to mature plant: *Arabidopsis* plastidial genome copy number, RNA accumulation and transcription are differentially regulated during leaf development. Plant Journal. 2007; 50:710–722. [PubMed: 17425718]

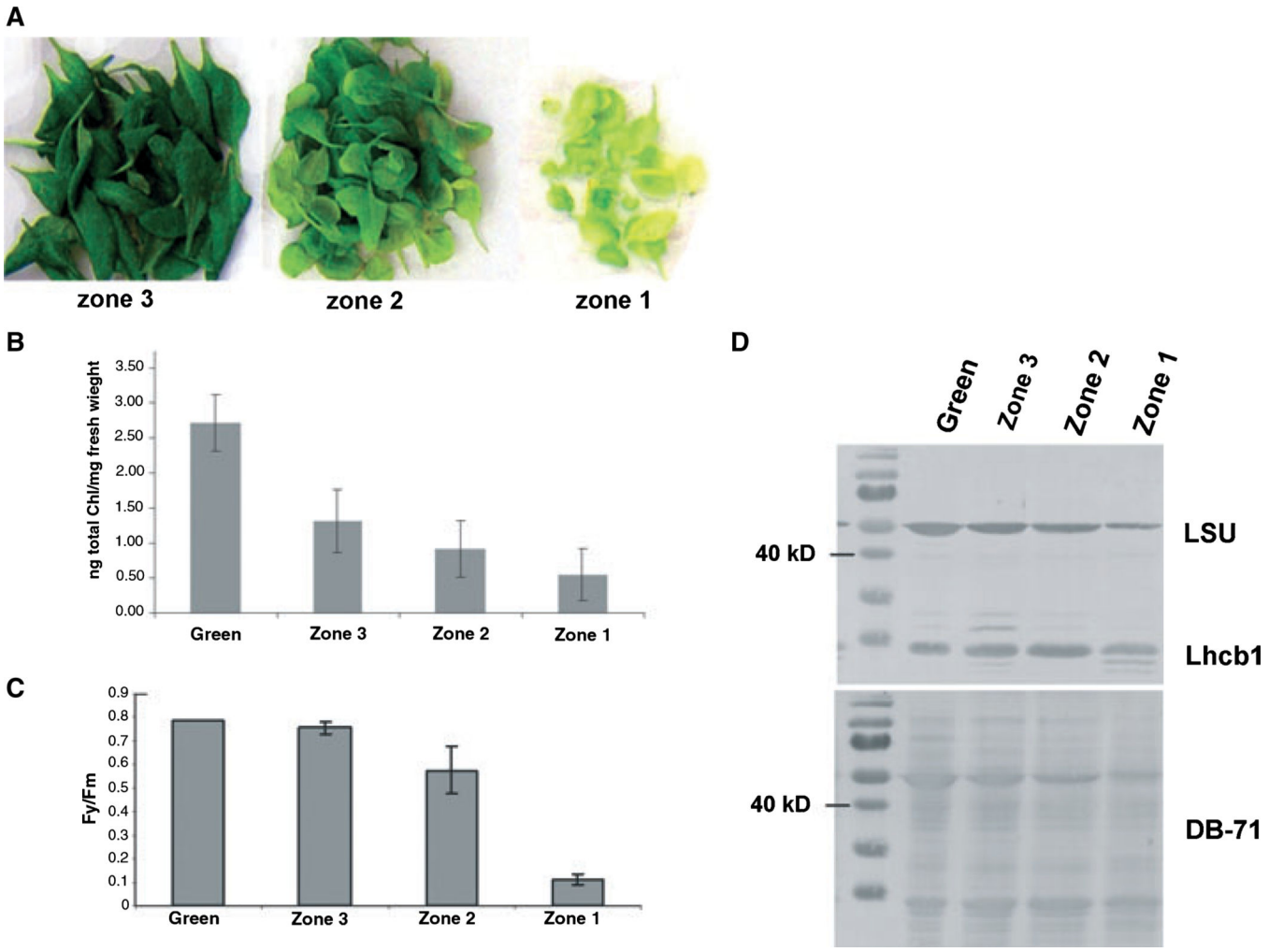

Fig. 1.

Zoning system for leaf senescence in *Arabidopsis*. A: Leaves were obtained from 7- to 8-week-old *Arabidopsis* rosettes, and separated into zones by visual inspection. Green tissue was harvested from mature leaves of 4-week-old plants while Zones 1–3 were harvested from 7- to 8-week-old plants. B: Total Chl was extracted from leaves (n = 8), and the average levels of Chl normalized to fresh weight ± SD are shown. C: Photochemical efficiency of photosytem II (Fv/Fm) was measured (n = 3), and the average values ± SD are shown. D: The levels of Rubisco LSU and Lhcb1 in each zone are shown in this immunoblot. Equal amounts of protein were loaded, as shown by DB-71 staining of the nitrocellulose filter prior to reaction with antibodies.

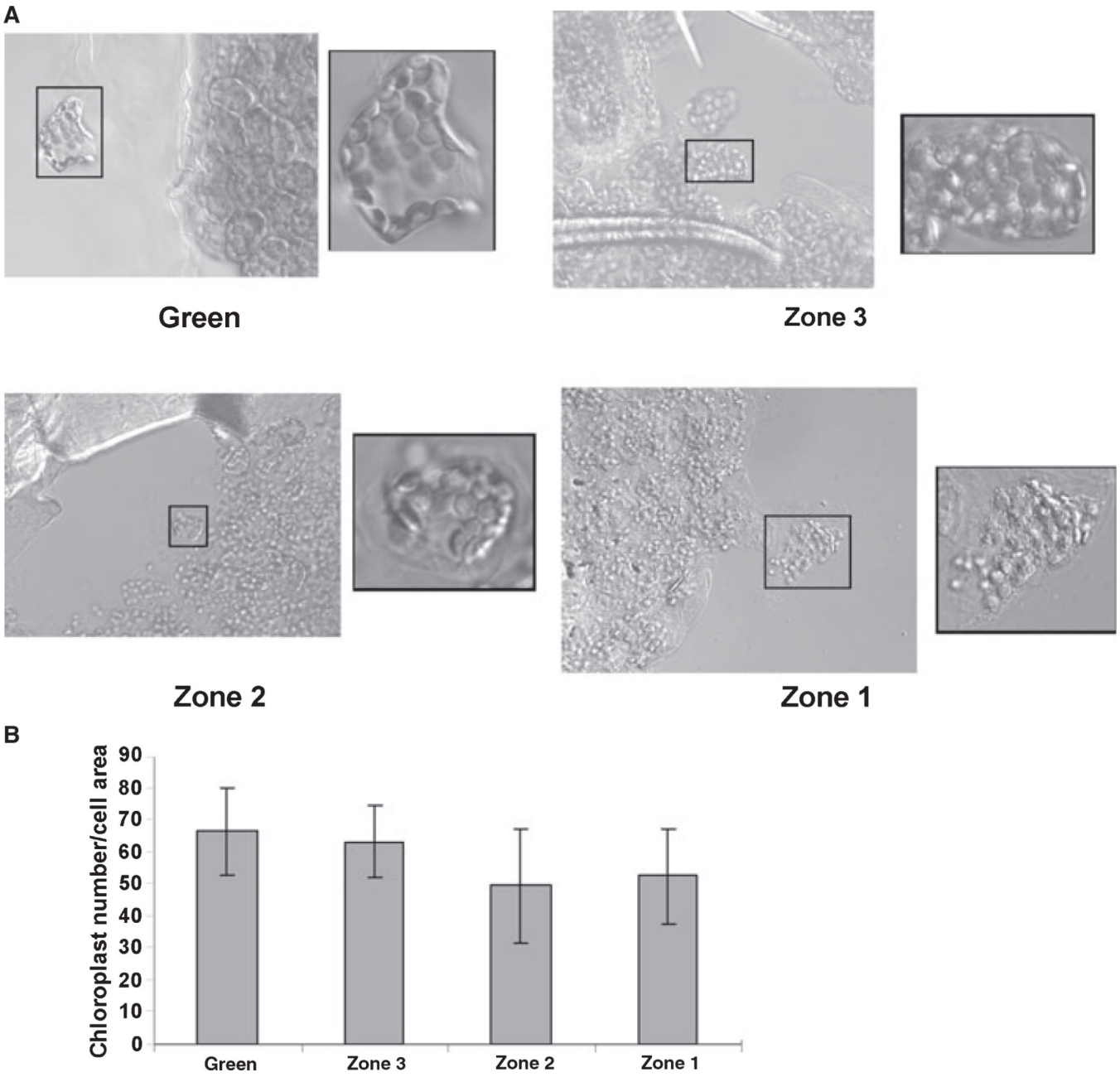

Fig. 2.

Chloroplast count per cell area. A: Mesophyll tissue was fixed, gently macerated, and then viewed by differential interference contrast microscopy. Chloroplasts were found to be plentiful in all zones observed. Higher magnification insets show chloroplasts at the surface of mesophyll cells. B: Chloroplasts were counted and then normalized to cell area (n = 16). Average values ± SD are shown.

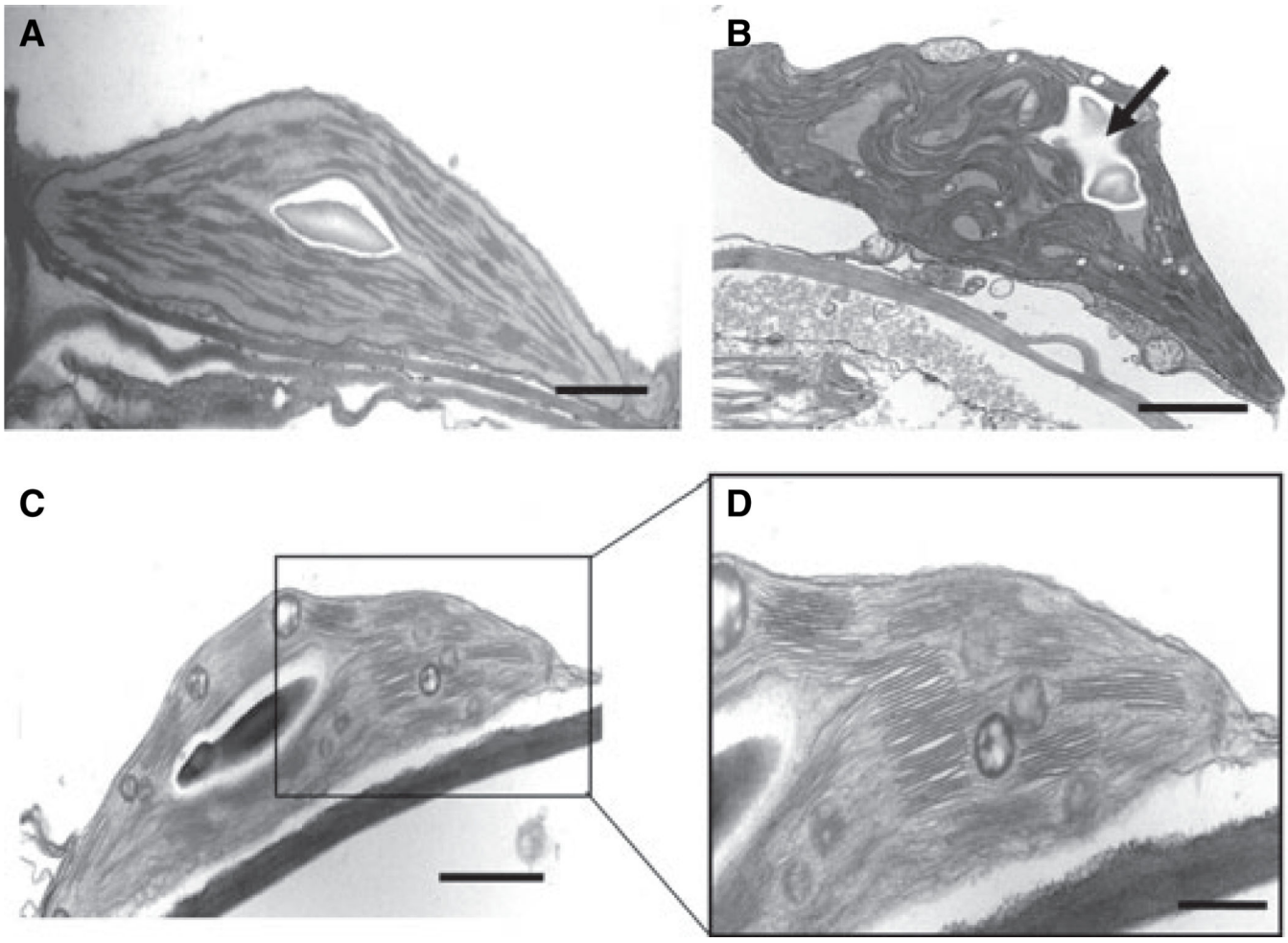

Fig. 3.

TEM micrographs of green, Zone 3, and Zone 2 tissues. A: A chloroplast from a green section has normal thylakoid membranes and a starch granule in the center; bar = 500 nm. B: A section from Zone 3 tissue showing swirling thylakoid membranes (top arrow) and a large starch granule; bar = 500 nm. C: Zone 2 tissue shows the coalescence of membranes into large, loose folds; bar = 500 nm. D: Higher magnification of (C); bar = 200 nm.

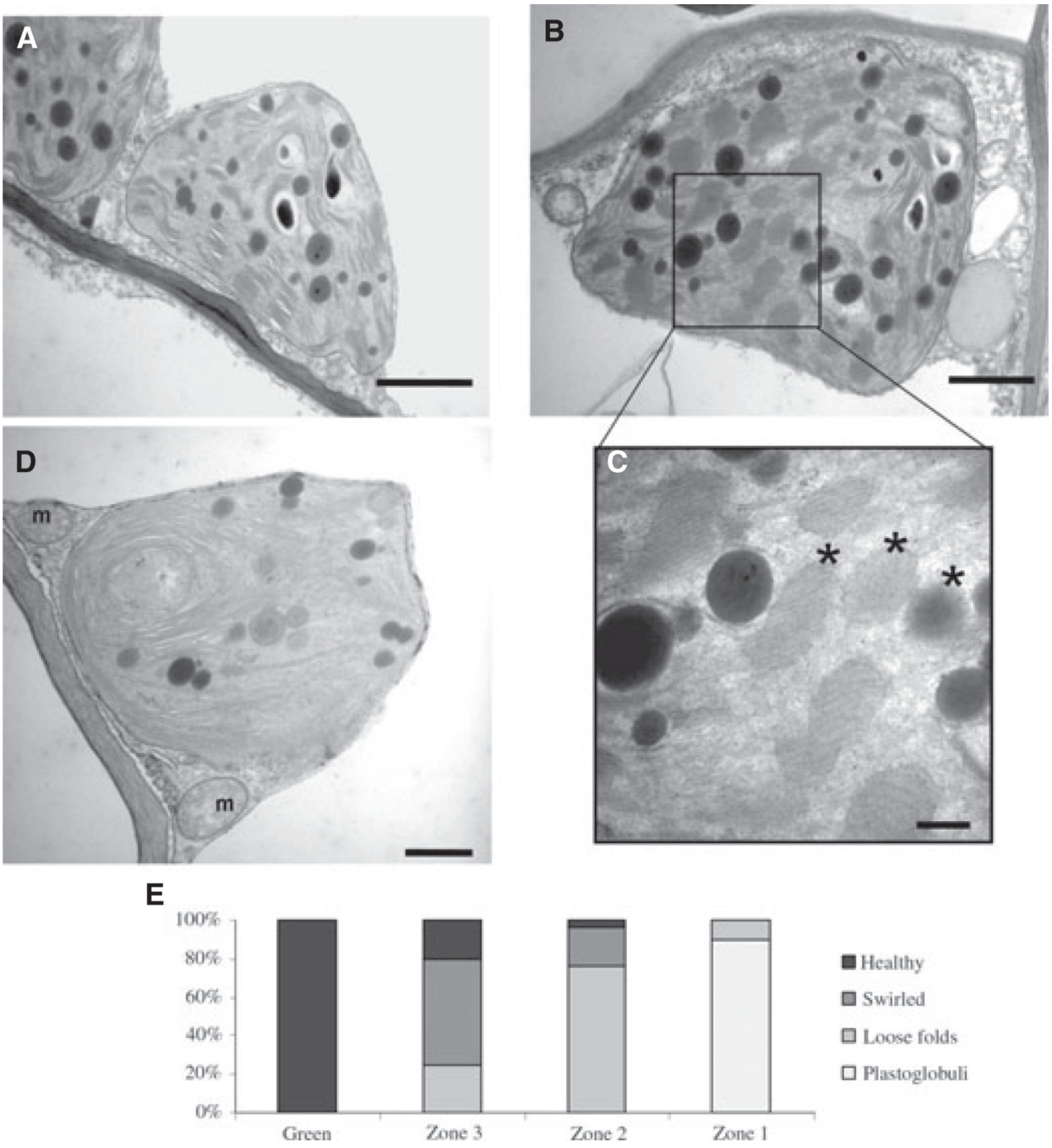

Fig. 4.

TEM micrographs of Zone 1 tissue and quantitation of chloroplast ultrastructure types in each zone. A: A chloroplast in Zone 1 has plastoglobuli and membrane folds; bar = 1000 nm. B: Circular membrane folds can be seen; bar = 200 nm. C: Higher magnification of (B) shows the loss of membrane folds and formation of more densely staining plastoglobuli, indicated by asterisks; bar = 100 nm. D: Intact, late-senescent chloroplast; mitochondria (m) are present and inner membranes appear normal; bar = 200 nm. E: Fifty chloroplasts from each zone were assigned an ultrastructure type, and tallies were plotted.

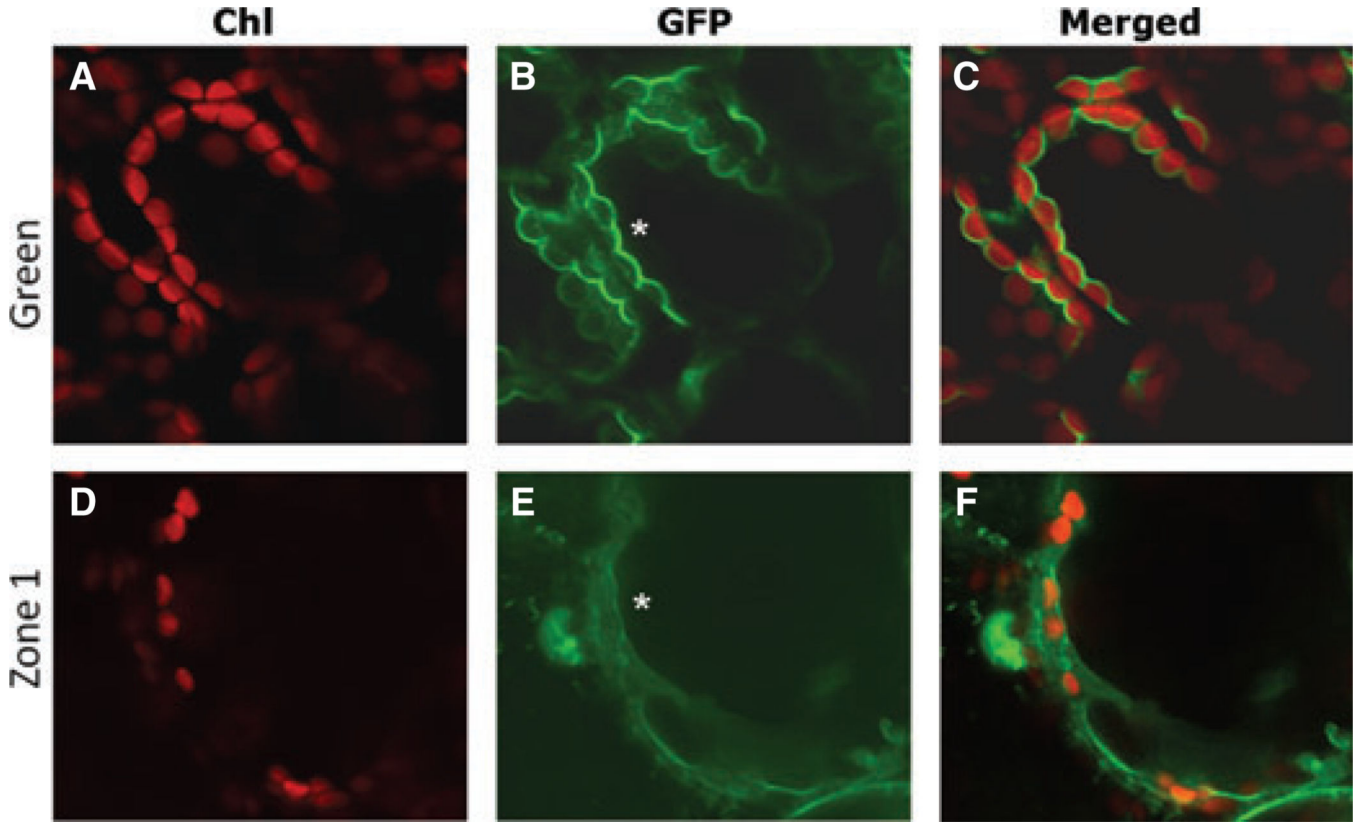

Fig. 5.

The 35S-GFP::δ-TIP line observed by confocal microscopy. Chl autofluorescence is observed in panels (A) and (D), GFP fluorescence is observed in panels (B) and (E), and the merged images can be seen in panels (C) and (F). Leaves from 4-week-old plants are shown in the top three panels, and yellow, Zone 1 leaves from 7-week-old plants are shown in the bottom three panels. Asterisks indicate regions where the tonoplast contours the chloroplasts.

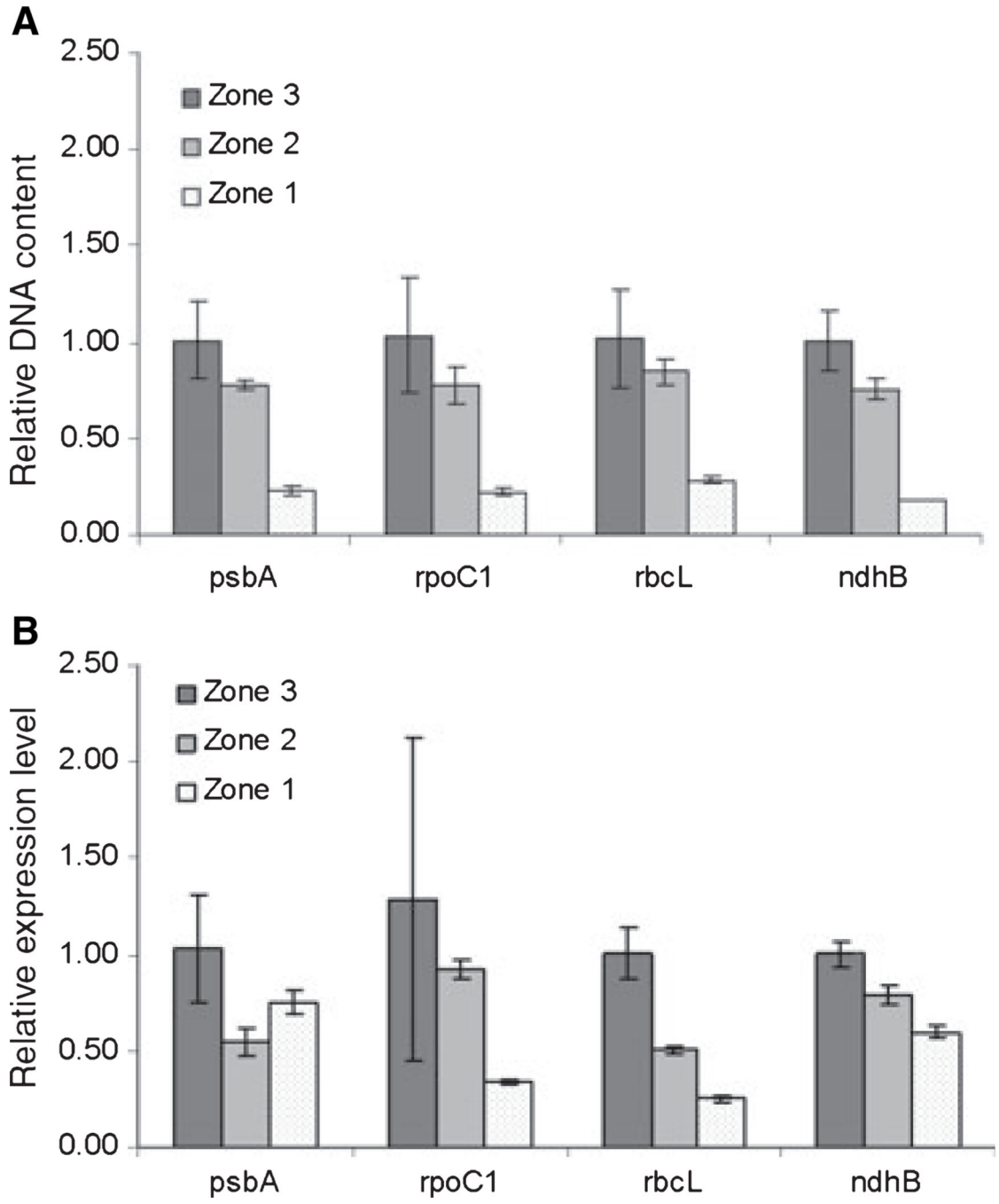

Fig. 6.

Real-time qPCR of nuclear and chloroplast DNA and cDNA. A: Genomic DNA was isolated from the three zones, and subjected to real-time PCR analysis using four chloroplast genes and one nuclear gene (Table 1). The nuclear gene served as a reference to control for equal loading, while Zone 3 served as the calibrator for $2^{-\Delta\Delta CT}$ analysis. The fold change in DNA content compared to Zone 3 leaves is shown, along with standard deviation. C_T values shown in Table 1 demonstrate that chloroplast DNA amplifies after far fewer PCR cycles than nuclear DNA. This experiment was repeated twice, and one representative experiment

is shown. B: RNA isolated from each zone was copied into cDNA, and used as a template for real-time qPCR. This experiment was repeated three times, and one representative experiment is shown.

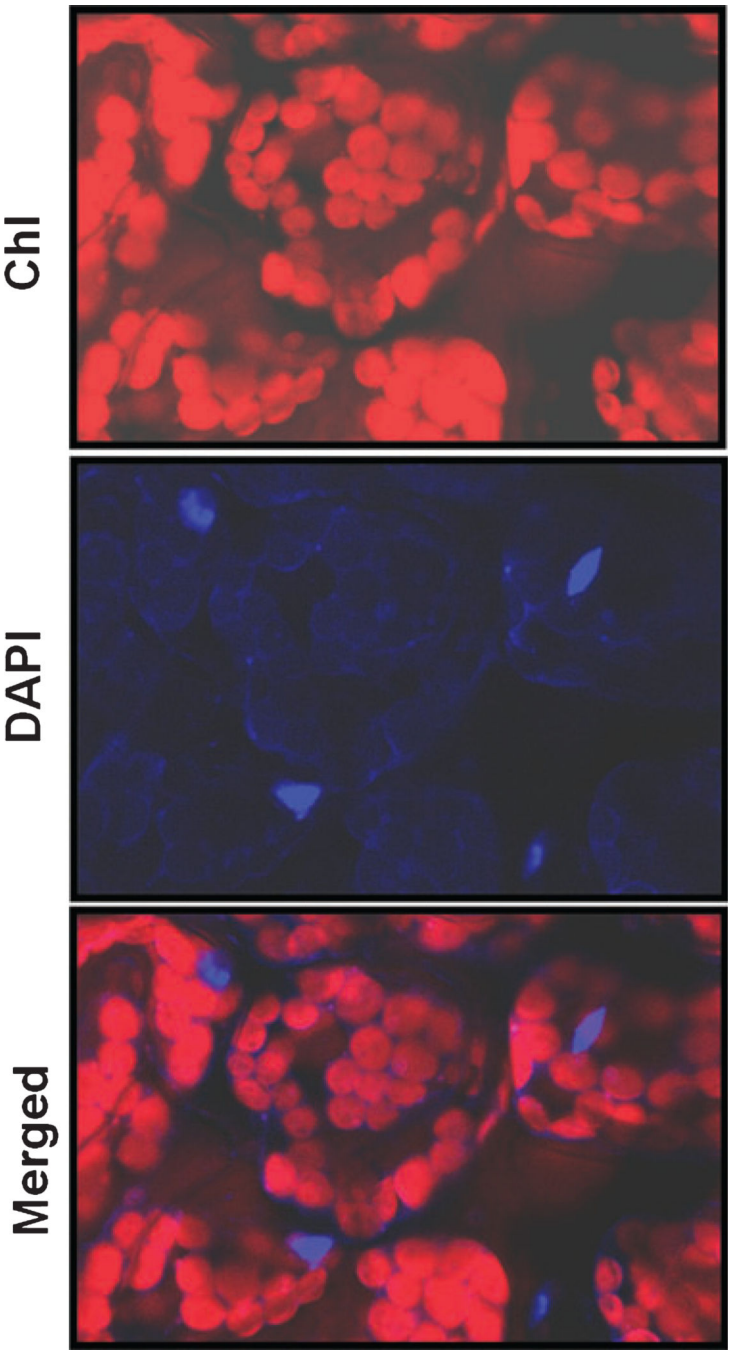

Fig. 7.

DAPI staining of mature *Arabidopsis* leaves. Leaves were fixed in glutaraldehyde and then stained with DAPI. The top panel shows Chl autofluorescence, the middle panel shows DAPI fluorescence, and the bottom panel is a merged image. Nuclei stained brightly with DAPI, while chloroplasts showed light staining, which was brightest at the periphery and outside of the chloroplast.

Table 1

Genes used in real-time PCR analysis, and C_T values for genomic DNA isolated from three different zones. Genes from four regions of the chloroplast genome were measured by real-time PCR, along with *actin2* (*ACT2*), a nuclear gene control. Duplicate copies of the *ndhB* gene are found on the chloroplast genome. C_T values were an average of three replicates. This experiment was repeated three times with similar results.

	psbA	**rpoC1**	**rbcL**	**ndhB.1 and ndhB.2**	**ACT2**
AGI name	AtCg00020	AtCg00180	AtCg00490	AtCg00890 AtCg01250	At3g18780
location on 154,478 bp Cp genome	383–1444	20251–23084	54958–56397	94941–96795 141854–143708	–
C_T Zone 3	13.8	12.8	13.7	13.0	20.2
C_T Zone 2	14.7	13.7	14.5	13.9	20.7
C_T Zone 1	16.8	15.8	16.4	16.3	21.0